Chapter 14
Activation Models for the Numerical Simulation of Cardiac Electromechanical Interactions

Ricardo Ruiz-Baier, Davide Ambrosi, Simone Pezzuto, Simone Rossi, and Alfio Quarteroni

Abstract This contribution addresses the mathematical modeling and numerical approximation of the excitation-contraction coupling mechanisms in the heart. The main physiological issues are preliminarily sketched along with an extended overview to the relevant literature. Then we focus on the existing models for the electromechanical interaction, paying special attention to the active strain formulation that provides the link between mechanical response and electrophysiology. We further provide some critical insight on the expected mathematical properties of the model, the ability to provide physiological results, the accuracy and computational cost of the numerical simulations. This chapter ends with a numerical experiment studying the electromechanical coupling on the anisotropic myocardial tissue.

14.1 Introduction

The interaction mechanism between contraction of the cardiac muscle and electrical propagation is a complex multiscale phenomenon of vital importance in a wide range of medical applications (Smith et al., 2004). From a purely mechanical point of view, key features of muscle behavior include large deformations, fiber anisotropy, heterogeneity of the tissue, and the ability to shorten when a substantial

R. Ruiz-Baier (✉) · S. Rossi · A. Quarteroni
CMCS-MATHICSE-SB, Ecole Polytechnique Fédérale de Lausanne, 1015 Lausanne, Switzerland
e-mail: ricardo.ruiz@epfl.ch

A. Quarteroni
e-mail: alfio.quarteroni@epfl.ch

S. Rossi
e-mail: simone.rossi@epfl.ch

D. Ambrosi · S. Pezzuto · A. Quarteroni
MOX—Politecnico de Milano, piazza Leonardo da Vinci 32, 20133 Milano, Italy

D. Ambrosi
e-mail: davide.ambrosi@polimi.it

S. Pezzuto
e-mail: simone.pezzuto@mail.polimi.it

G.A. Holzapfel, E. Kuhl (eds.), *Computer Models in Biomechanics*,
DOI 10.1007/978-94-007-5464-5_14,

intracellular calcium concentration change occurs. The dynamics is driven by a traveling action potential, usually modeled by a reaction-diffusion equation, where the ions species diffusion activates the ionic currents reaction, which eventually dictate the depolarization and repolarization of the cells. Ionic currents depend on the jump in electric potential according to Ohm's law whereas the conductance is typically a highly nonlinear function of voltage described through gating variables or, more recently, by means of Markov models. Such a nonlinearity is responsible for the complex excitable behavior of the cardiac action potential cycle: rapid upstroke of depolarization, followed by a plateau phase and a repolarization of the cells when a voltage threshold is overcome. A variety of models exists in this respect, with increasing detail in the description of ionic channels and intracellular reactions taken into account (CellML, 2000; Rudy and Silva, 2006). Heuristic systems of equations, that only reproduce a qualitative pattern of the voltage wave, are very useful in providing a framework simple enough to allow for mathematical analysis. However, these kind of phenomenological models are not able to describe the correct behavior of the cell in a pathological condition, or correctly describe drug interactions; furthermore, the concentration of specific ions like intracellular calcium that induces contractions and relaxations of cardiomyocytes, is typically not present. Therefore a more detailed insight of several ionic currents is needed to provide the correct physiological contractility.

The numerical simulation of these complex multiphysics and multiscale systems poses a major challenge even if state-of-the-art computational techniques and computer architectures are employed. Finite element formulations of nonlinear elasticity for the myocardial tissue have been proposed since more than a decade (Nash and Hunter, 2000), followed by a series of works focusing on the integration of cardiac systems including elasticity, electricity, perfusion models, and on the close connection of the proposed models with experimental observations (see a review in Kerckhoffs et al., 2006). If a certain level of accuracy of the geometrical description of a patient specific model is desired and the solution is to be obtained within a reasonable amount of time, there is no way around using parallel computers (and suitable numerical techniques combined with scalable algorithms exploiting the underlying architectures). The public availability of scientific computing libraries such as, e.g., LifeV (2001), Continuity (2005) and Chaste (Pitt-Francis et al., 2009), represents a substantial step forward in this direction. Parallel algorithms capable of performing cardiac mechano-electrical simulations have recently been implemented reporting scalable behaviors in Chapelle et al. (2009); Reumann et al. (2009); Lafortune et al. (2012); Nobile et al. (2012).

In this paper we aim at investigating some features of the active strain formulation in cardiac electromechanics (Cherubini et al., 2008; Ambrosi et al., 2011; Nobile et al., 2012). Such approach is based on the assumption that the mechanical activation, laying in the core of the cell-level excitation-contraction mechanism, may be represented as a virtual multiplicative splitting of the deformation gradient into a passive elastic response, and an active deformation depending directly on the electrophysiology. Alternative options that avoid such decomposition at the deformation level are active-stress descriptions (see, e.g., Nash and Panfilov, 2004;

Pathmanathan and Whiteley, 2009; Land et al., 2012) where the stress is composed as a sum of a passive and an active part, the latter determined by the so-called active tension, also depending on the electrical activation of the cell. In this paper we address the feasibility of numerical simulations for the macroscopic coupling using the active strain approach, and we present in detail an example of the full electromechanical interaction. However, we will not discuss advantages and disadvantages of the different strategies, rather we refer to Ambrosi and Pezzuto (2012) and Rossi et al. (2012) for a thorough comparison.

This paper is organized as follows. In Sect. 14.2 we summarize the main mathematical characteristics of the electrical and mechanical problem and we detail the specific modeling strategy that we adopt. The electromechanical coupling, i.e. the cell contraction dictated by the electrical signal and the corresponding feedback (the stretch activated currents) are illustrated in Sect. 14.3. The computational method is outlined in Sect. 14.4 where we also present a numerical example, and we close with a discussion in Sect. 14.5.

14.2 Mathematical Models for Cardiac Electromechanics

Force balance equations for an elastic continuum medium are employed to describe large deformations of the myocardium under influence of the fluid pressure, the surrounding organs and its own contraction. Such framework has to be coupled with the macroscopic bidomain or monodomain equations accounting for the propagation of the electric potential and ionic currents.

14.2.1 Models for the Heart Electrophysiology

Starting from the pioneering work of Hodgkin and Huxley (1952) on the nerve axon model, several increasingly sophisticate models have been developed for the propagation of electrical signals in cardiac tissue. Here we separate between models for cardiac cell electrophysiology, and macroscopic tissue-level models based on continuum mechanics.

Popular cardiac cellular electrophysiology models include those based on experimental observations on animals (e.g., Luo and Rudy, 1991) and humans (see, e.g., Iyer et al., 2004; ten Tusscher et al., 2004). Such models address cell excitation in isolation from the rest of the cardiac function. They essentially include a description of the dynamics of ionic species (mainly potassium, calcium, and sodium) along with the gating processes of several proteins that are blocked or allowed to transport ions through the cellular membrane. A drastic decrease of computational cost can be obtained by using simplified low dimensional models based on phenomenological descriptions of such mechanisms (Rogers and McCulloch, 1994; Bueno-Orovio et al., 2008). The price to pay for this simplification, provided that a correct behavior of

the voltage field is reproduced, is that ionic species are not well resolved. Nevertheless, these types of electrical models are able to provide some specific information of interest, such as contractility.

Systems of ordinary differential equations (ODEs) of the form

$$\partial_t v - I_{\text{ion}}(v, \mathbf{w}) = 0, \qquad \partial_t \mathbf{w} - \mathbf{m}(v, \mathbf{w}) = \mathbf{0}, \tag{14.1}$$

are employed to describe these cellular models, without any spatial detail. Here v denotes the transmembrane potential field, $\mathbf{w}$ contains all gating variables and concentration of ionic species, and I_{ion} and $\mathbf{m}$ drive the kinetics of the system, its specific form depending on the chosen cellular model.

Models at the cell level can be incorporated into macroscopic descriptions for the propagation of electrical excitation throughout the cardiac muscle in the simplest way assuming homogeneous diffusion of ionic species on the microstructure of the substrate. The texture of the cardiac tissue can be incorporated observing that cellular and extracellular components are characterized by different diffusivities. A homogenization process yields the so-called bidomain equations (Tung, 1978):

$$\partial_t v - \nabla\cdot(\mathbf{D}_{\text{e}}\nabla u_{\text{e}}) + I_{\text{ion}} = I^{\text{i}}_{\text{app}}, \qquad \partial_t v + \nabla\cdot(\mathbf{D}_{\text{i}}\nabla u_{\text{i}}) + I_{\text{ion}} = I^{\text{e}}_{\text{app}}, \tag{14.2}$$

where u_{i} and u_{e} are the intra- and extracellular electric potentials (both defined in every point of the domain), and $(I^{\text{i}}_{\text{app}}, I^{\text{e}}_{\text{app}})$ are possible externally applied stimuli.

The cardiomyocytes are organized in fibers that originate the anisotropic conductivity in the electrophysiology of the heart. The myofiber angle varies continuously from about $-60°$ (inverse circumferential axis) at the epicardium, to about $70°$ at the endocardium. From the apical region, the myofibers that conform the tissue follow a right helical orientation towards the subendocardium and a left helical path parallel to the wall on the subepicardium. On the mid-wall region, cardiac fibers exhibit a circumferential orientation, and on the basal site fibers cross from subendocardial to the subepicardial region. Myocardial propagation velocities in the parallel and perpendicular myofiber directions can differ up to an order of magnitude. These geometrical features are encoded in the anisotropic conductivity tensors $\mathbf{D}_{\text{i}}$ and $\mathbf{D}_{\text{e}}$ (Colli Franzone and Pavarino, 2004).

14.2.2 Mechanical Response of the Myocardium

The characterization of the material properties of the cardiac tissue requires precise experimental settings that should reproduce physiological conditions as close as possible. Usual tests include uniaxial and biaxial tension experiments, as well as shear tests, from which it is possible to recover stress-strain relations on the different directions of the anisotropic medium (fiber, sheets, and sheet-normal axes).

The usual kinematics descriptors of a continuum medium placed in $\Omega_{\text{o}} \subset \mathbb{R}^3$ in its reference configuration are the deformation gradient of its motion $\mathbf{F}$ and the

right Cauchy-Green tensor $\mathbf{C} = \mathbf{F}^{\mathrm{T}}\mathbf{F}$. We denote by $I_1 = \operatorname{tr}\mathbf{C}$, $I_2 = \frac{1}{2}(I_1^2 - \operatorname{tr}\mathbf{C}^2)$, $I_3 = \det\mathbf{C}$, the principal invariants of $\mathbf{C}$.

Due to the alignment of cardiac fibers and their organization in sheets, the myocardium exhibits an orthotropic behavior that can be conveniently illustrated introducing the orthogonal unit vector fields $\mathbf{f}_0$ and $\mathbf{s}_0$ denoting the orientation of the fibers and collagen-sheets in the reference configuration. A hyperelastic material with constitutive response invariant with respect to rotations around $\mathbf{f}_0$ and $\mathbf{s}_0$ is described by a strain-energy function $\mathscr{W}(\mathbf{F})$ that depends on a set of invariant such as $I_{1,2,3}$, and also pseudo-invariants defined as follows:

$$I_{4,f} = \mathbf{C} : \mathbf{f}_0 \otimes \mathbf{f}_0, \qquad I_{5,f} = \mathbf{C}^2 : \mathbf{f}_0 \otimes \mathbf{f}_0, \qquad I_{8,fs} = \mathbf{C} : \operatorname{sym}(\mathbf{f}_0 \otimes \mathbf{s}_0), \quad (14.3)$$

and analogously $I_{4,s}$ and $I_{5,s}$.

Orthotropic strain-energy functions were suggested in Usyk et al. (2000); Costa et al. (2001); Holzapfel and Ogden (2009), that in addition are able to represent the behavior of the laminar sheets in which cardiac myofibers are structured. For instance, the energy function proposed by Holzapfel and Ogden (2009) is given by

$$\mathscr{W}(\mathbf{F}) = \frac{a}{2b}\left(\mathrm{e}^{b(I_1-3)} - 1\right) + \sum_{i=f,s} \frac{a_i}{2b_i}\left(\mathrm{e}^{b_i(I_{4,i}-1)^2} - 1\right) + \frac{a_{fs}}{2b_{fs}}\left(\mathrm{e}^{b_{fs}I_{8,fs}^2} - 1\right), \quad (14.4)$$

where the eight parameters a, b, a_f, b_f, a_s, b_s, a_{fs} and b_{fs} are experimentally fitted.

According to Ashikaga et al. (2008), the myocardium experiments a change in myocardial volume of up to 10 %. This is possibly due to blood-filled spaces within the myocardium which may communicate with the ventricular lumen or from the coronary arteries from which blood is expelled during systole. However incompressibility of the medium is often assumed as it is mainly constituted by water. In strictly incompressible models, the pressure field is the Lagrange multiplier enforcing the constraint, and in slightly compressible models a compressibility modulus penalizes the variation in density. For evident reasons, strict incompressibility is more popular when analytical methods are applied, as one degree of freedom drops out in homogeneous deformations, while penalization is often preferred in numerical codes, where no compatibility between spaces of representation of displacement and pressure fields must be abided.

14.3 Activation and Contraction

Myocardial systolic contraction is usually modeled at the macroscale by incorporating a possibly anisotropic, additive stress contribution in the force balance (Nash and Panfilov, 2004; Smith et al., 2004; Göktepe and Kuhl, 2010; Pathmanathan et al., 2010).

A different approach is to introduce a multiplicative decomposition of the strain. The active strain method, introduced in the context of biomechanics in Taber and

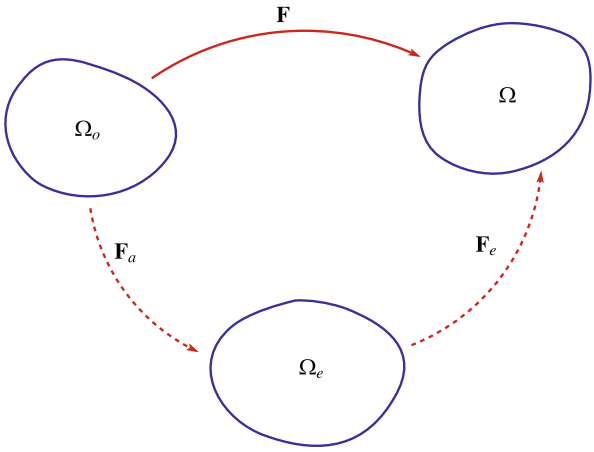

Fig. 14.1 Sketch of the active strain decomposition entailing an intermediate virtual configuration Ω_e between the reference state Ω_o and the current configuration Ω. Similar splittings have been proposed in finite elastoplasticity (Lee and Liu, 1967), growth and material remodeling (Taber and Perucchio, 2000; Menzel and Waffenschmidt, 2009), and mechano-chemical interactions (Murtada et al., 2010)

Perucchio (2000); Nardinocchi and Teresi (2007), assumes that the deformation gradient $\mathbf{F}$ can be rewritten in terms of a Lee-type multiplicative decomposition (Lee and Liu, 1967), i.e.

$$\mathbf{F} = \mathbf{F}_e \mathbf{F}_o, \tag{14.5}$$

where $\mathbf{F}_o$ is the active deformation, to be constitutively prescribed in terms of ionic species concentration, and $\mathbf{F}_e$ is the passive elastic deformation (see Fig. 14.1). Whichever approach that is chosen, the model should satisfy due mathematical properties (such as frame indifference and ellipticity of the total stress), and the constitutive laws need to recover physiological relevant behaviors (such as the Frank-Starling effect, where an increase of chamber volume at end-systolic pressure and stroke work reflects on the tissue as a monotonic increase in isometric tension), (Lee and Liu, 1967).

Comparisons between the usual active stress method and the active strain approach from a numerical viewpoints has been carried out in Rossi et al. (2012). Defining the variables γ_f, γ_s, γ_n as the relative displacements in the directions $\mathbf{f}_0$, $\mathbf{s}_0$, $\mathbf{n}_0$, (fibers, sheets and sheets-normal directions) of a single cell, respectively, the *local* deformation is

$$\mathbf{F}_o = \mathbf{I} + \gamma_f \mathbf{f}_0 \otimes \mathbf{f}_0 + \gamma_s \mathbf{s}_0 \otimes \mathbf{s}_0 + \gamma_n \mathbf{n}_0 \otimes \mathbf{n}_0. \tag{14.6}$$

Note that γ_f represents the active shortening of the cardiomyocytes, whereas γ_s, γ_n will take into account the associated thickening, in order to satisfy the incompressibility of the cell itself (Iribe et al., 2007; Smerup et al., 2009). In Nardinocchi and Teresi (2007), Evangelista et al. (2011) and Nobile et al. (2012), the contribution of the terms depending on γ_s and γ_n are not included. Analogously, for some activation models (see, e.g., Göktepe and Kuhl, 2010; Rausch et al., 2011), the active tension is assumed to act exclusively along the fibers direction. However, biaxial tests provide a measure of the active contributions in the transverse direction. This quantification can be obtained by either measuring the different rates of calcium

release in these directions (as done in Usyk et al., 2000) and then translating this information into active strains, or assuming transverse isotropy of the mechanical response at the cell level (as in Rossi et al., 2012). Moreover, if the components of the activated deformation $\mathbf{F}_\mathrm{o}$ satisfy the condition

$$(1+\gamma_f)(1+\gamma_s)(1+\gamma_n)=1, \tag{14.7}$$

then $\det\mathbf{F}_\mathrm{o}\equiv 1$, a very convenient choice from a numerical point of view for this nonlinear problem, since convergence has to be incrementally reached.

The thermodynamic assumption of the multiplicative decomposition (14.5) is that the active deformation $\det\mathbf{F}_\mathrm{o}$ stores no energy, so that the strain-energy function is $\widehat{\mathscr{W}}=\mathscr{W}(\mathbf{F}_\mathrm{e})$ and

$$\mathscr{W}_{\mathrm{strain}}=\det\mathbf{F}_\mathrm{o}\,\widehat{\mathscr{W}}=\det\mathbf{F}_\mathrm{o}\,\mathscr{W}\left(\mathbf{F}\mathbf{F}_\mathrm{o}^{-1}\right). \tag{14.8}$$

The activation γ_f depends on the concentration of ionic species as can be deduced from ordinary differential equation models (Rice et al., 2008; Murtada et al., 2010; Nobile et al., 2012), which can be summarized in the symbolic equation

$$\partial_t\gamma_f-G(\mathbf{w},\gamma_f)=0, \tag{14.9}$$

where G defines the activation dynamics depending on ionic concentrations denoted by the vector $\mathbf{w}$.

In the reference configuration Ω_o, the equations governing the electromechanical interaction under active strain read

$$\begin{cases} -\nabla\cdot\left(\det\mathbf{F}_\mathrm{o}\dfrac{\partial\mathscr{W}(\mathbf{F}\mathbf{F}_\mathrm{o}^{-1})}{\partial\mathbf{F}}-p\mathbf{F}^{-T}\right)=0, & \text{in } \Omega_\mathrm{o};\\ \det\mathbf{F}=1,\\ \chi c_\mathrm{m}\partial_t v-\nabla\cdot\left(\mathbf{F}^{-1}\mathbf{D}_\mathrm{e}\mathbf{F}^{-T}\nabla u_\mathrm{e}\right)+\chi(I_\mathrm{ion}+I_\mathrm{sac})=I_\mathrm{app}^\mathrm{i},\\ \chi c_\mathrm{m}\partial_t v+\nabla\cdot\left(\mathbf{F}^{-1}\mathbf{D}_\mathrm{i}\mathbf{F}^{-T}\nabla u_\mathrm{i}\right)+\chi(I_\mathrm{ion}+I_\mathrm{sac})=I_\mathrm{app}^\mathrm{e}, & \text{in } \Omega_\mathrm{o}\times(0,T).\\ \partial_t\mathbf{w}-\mathbf{m}(v,\mathbf{w})=0,\\ \partial_t\gamma_f-G(\mathbf{w},\gamma_f)=0, \end{cases} \tag{14.10}$$

System (14.10) is to be completed with suitable initial data for v, $\mathbf{w}$ as well as with boundary conditions for all fields. The usual prescription of voltage at the initial time is that a large enough perturbation is located at the apex, so that an electric wave starts traveling up to the base, producing the due ionic currents and mechanical contraction. This initial condition corresponds to immaterial assumption that the electric signal, actually produced at the sinoatrial node, has been traveling very fast along the Purkinje fibers down to the apex, where they finely branch producing a volumetric diffusion at $t=0$. Since the Purkinje fibers also branch up from the apex towards the base at the subepicardial level, different protocols are often used to

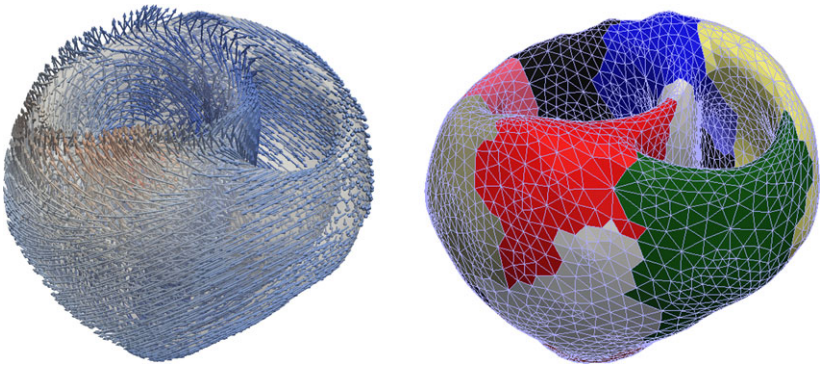

Fig. 14.2 Fiber distribution on the myocardium (*left panel*), and sketch of the geometrical domain decomposition of the corresponding mesh into 16 subdomains (*right panel*)

stimulate the entire endocardial surface. This is done either synchronously or with a slight delay going from apex to base. No-flux boundary conditions apply to the electric variables, while mixed boundary data are imposed to the displacement field. Robin conditions mimic the presence of the pericardial sac at the outer wall, while blood pressure inside the ventricles is computed on the basis of pressure-volume diagrams, relating the blood pressure depending to the ventricular volume.

14.4 Numerical Simulation

In what follows we present a simple numerical example illustrating the feasibility of electromechanical active strain models. The simulations reported in the present work are performed using the parallel finite element library LifeV (2001). We employed a biventricular geometry (originally from Sermesant, 2003) where the mesh consists of 29 504 tetrahedral elements. Myocardial fibers are distributed in the muscle following an analytical description so that the orientation varies linearly from an elevation angle (between the short axis plane and the fiber) of 65° in the epicardium, to −65° in the endocardium (see Fig. 14.2, left panel). The domain is then partitioned into 16 subdomains (Fig. 14.2, right panel).

Since we are interested in the myocardium activation more than the passive properties of the muscle, we consider a simple neo-Hookean material with strain-energy function $\mathscr{W} = \frac{\mu}{2}\mathbf{F} : \mathbf{F}$, where $\mu = 385$ kPa, in all regions of the cardiac muscle. Moreover, the active strain $\mathbf{F}_o$ is chosen to be transversely isotropic, so $\gamma_s = \gamma_n = 0$ and therefore condition (14.7) is not needed. This means that the second Piola-Kirchhoff tensor reads:

$$\mathbf{S} = \mu(1-\gamma_f)\mathbf{I} + \mu\gamma_f \frac{2-\gamma_f}{1-\gamma_f}\mathbf{f}_0 \otimes \mathbf{f}_0. \tag{14.11}$$

The specifications for (14.1) are in accordance with the minimal model of Bueno-Orovio et al. (2008), a four-equations phenomenological model for human ventricles. The auxiliary variables are $\mathbf{w} = (w_1, w_2, w_3)$ which are phenomenological quantities (no direct physical interpretation), however w_3 behaves like a re-scaled intracellular calcium concentration. The reaction terms are defined as

$$I_{\text{ion}}(v, \mathbf{w}) = -w_1 H(v-\theta_1)(v-\theta_1)(v_v - v)/\tau_{fi} + (v - v_0)\big(1 - H(v-\theta_2)\big)/\tau_0 + H(v-\theta_2)/\tau_{3,0} - H(v-\theta_2)w_2 w_3/\tau_{si}, \tag{14.12}$$

and

$$\mathbf{m}(v, \mathbf{w}) = \begin{pmatrix} ((1 - H(v-\theta_1))(w_{1,\text{inf}} - w_1)/\tau_1^- - H(v-\theta_1)w_1/\tau_1^+ \\ (1 - H(v-\theta_2))(w_{2,\text{inf}} - w_2)/\tau_2^- - H(v-\theta_2)w_2/\tau_2^+ \\ ((1 + \tanh(k_3(v - v_3)))/2 - w_3)/\tau_3)^{\mathrm{T}} \end{pmatrix}, \tag{14.13}$$

where H stands for the usual Heaviside function. The switches and infinite values are defined as follows:

$$\tau_1^- = \big(1 - H\big(v - \theta_1^-\big)\big)\tau_{1,1}^- + H\big(v - \theta_1^-\big)\tau_{1,2}^- \tag{14.14}$$

$$\tau_2^- = \tau_{2,1}^- + \big(\tau_{2,2}^- - \tau_{2,1}^-\big)\big(1 + \tanh\big(k_2^-\big(v - v_2^-\big)\big)\big)/2 \tag{14.15}$$

$$\tau_{3,0} = \tau_{3,0,1} + (\tau_{3,0,2} - \tau_{3,0,1})\big(1 + \tanh\big(k_{3,0}(v - v_{3,0})\big)\big)/2 \tag{14.16}$$

$$\tau_3 = \big(1 - H(v-\theta_2)\big)\tau_{3,1} + H(v-\theta_2)\tau_{3,2} \tag{14.17}$$

$$\tau_0 = \big(1 - H(v-\theta_0)\big)\tau_{0,1} + H(v-\theta_0)\tau_{0,2} \tag{14.18}$$

$$w_{1,\text{inf}} = \begin{cases} 1, & v < \theta_1^- \\ 0, & u \geq \theta_1^- \end{cases} \tag{14.19}$$

$$w_{2,\text{inf}} = \big(1 - H(v-\theta_0)\big)(1 - v/\tau_{2,\infty}) + H(v-\theta_0)w_{2,\infty}^*. \tag{14.20}$$

The model reproduces the correct shape of the voltage wave. For the sake of simplicity, we use the epicardial parameters for the whole cardiac muscle: $\theta_0 = 0.005$, $\theta_1 = 0.3$, $\theta_2 = 0.13$, $\theta_1^- = 0.1$, $\tau_{3,0,1} = 91$, $\tau_{3,0,2} = 0.8$, $\tau_{3,1} = 2.7342$, $\tau_{3,2} = 4$, $\tau_{0,1} = 410$, $\tau_{0,2} = 7$, $w_{2,\infty}^* = 0.5$, $v_v = 1.61$, $\tau_{1,1}^- = 80$, $\tau_{1,2}^- = \tau_1^+ = 1.4506$, $\tau_{2,1}^- = 70$, $\tau_{2,2}^- = 8$, $\tau_2^+ = 280$, $k_2^- = 200$, $v_2^- = 0.016$, $\tau_{fi} = 0.078$, $k_{3,0} = 2.1$, $v_{3,0} = 0.6$, $k_3 = 2.0994$, $v_3 = 0.9087$, $\tau_{si} = 3.3849$, $\tau_{2,\infty} = 0.01$. The initial data corresponds to $w_1 = w_2 = 1$, $w_3 = 0$.

The governing ODE for the activation corresponds to (14.9), as introduced in Rossi et al. (2011) and Nobile et al. (2012), with the specification $G(\gamma_f, w_3) = -0.02w_3 - 0.04\gamma_f$.

The time sequence of transmembrane potential, activation γ_f and other ionic concentrations are illustrated in Fig. 14.3 for a point on the epicardial surface. The highest activation value is attained with a delay of about 120 ms with respect to that of the action potential.

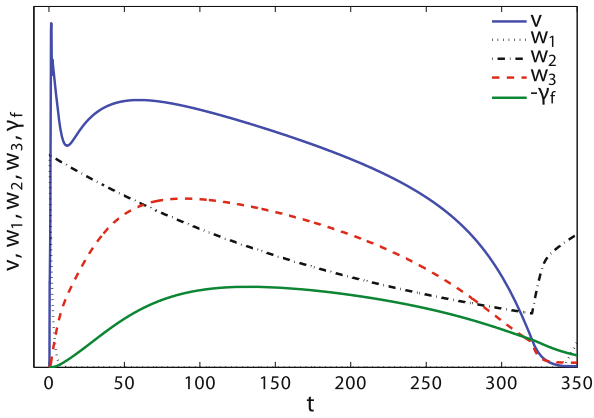

Fig. 14.3 Time evolution of the electric fields in a specific epicardial position of the tissue. Plotted quantities are the transmembrane potential v, gate variables $\mathbf{w} = (w_1, w_2, w_3)$ and the mechanical activation γ_f which are all presented in dimensionless form

Robin boundary condition $m\mathbf{u} + \mathbf{Pn} = \mathbf{0}$, with $m = \mu = 385$ kPa, has shown to yield a qualitatively correct end-systolic displacement magnitude (around 25 %) and rotation of the left ventricle, as reported in Rossi et al. (2012). Quadratic finite elements are used for displacement, whereas all other fields are discretized using continuous piecewise trilinear elements, in order to satisfy Brezzi-Babuška *inf-sup* condition. The timestep, fixed during the simulation, is $\Delta t = 0.01$ ms and, as usual in electromechanically coupled computational models (see, e.g., Nash and Panfilov, 2004; Cherubini et al., 2008; Pathmanathan and Whiteley, 2009; Land et al., 2012), we iterate between electrical and mechanical problems in a segregated mode. The nonlinear equations arising from the discretization of the mechanical problem are linearized using the Newton-Raphson method. We find that no more than 6 iterations are needed to converge with a tolerance of $\varepsilon_{\text{tol}} = 10^{-8}$, with the maximum number of iterations being always attained around the upstroke phase. The linear systems are solved using the GMRES iterative method (with a tolerance of $\hat{\varepsilon}_{\text{tol}} = 10^{-7}$). The average overall CPU time spent per time step is 3.5 seconds, using 32 cores distributed on 4 nodes on the Intel Harpertown cluster *Callisto* at EPFL.[1]

An external stimulus $I^{\text{e}}_{\text{app}} = -100$ μA is applied at the apex at $t = 0$, in order to generate a traveling wave for the transmembrane potential, initially everywhere at rest ($v = -84$ mV). Figure 14.4 presents three snapshots of the solution of the excitation-contraction problem at times $t = 1$, $t = 40$, $t = 230$ and $t = 540$ ms, where fiber directions are represented by the gray volume arrows and the color-map shows the values of the transmembrane potential v on the undeformed solid. Notice that the activation patterns adopt a profile dictated by the tissue anisotropy.

[1] http://hpc-dit.epfl.ch/clusters/callisto.php.

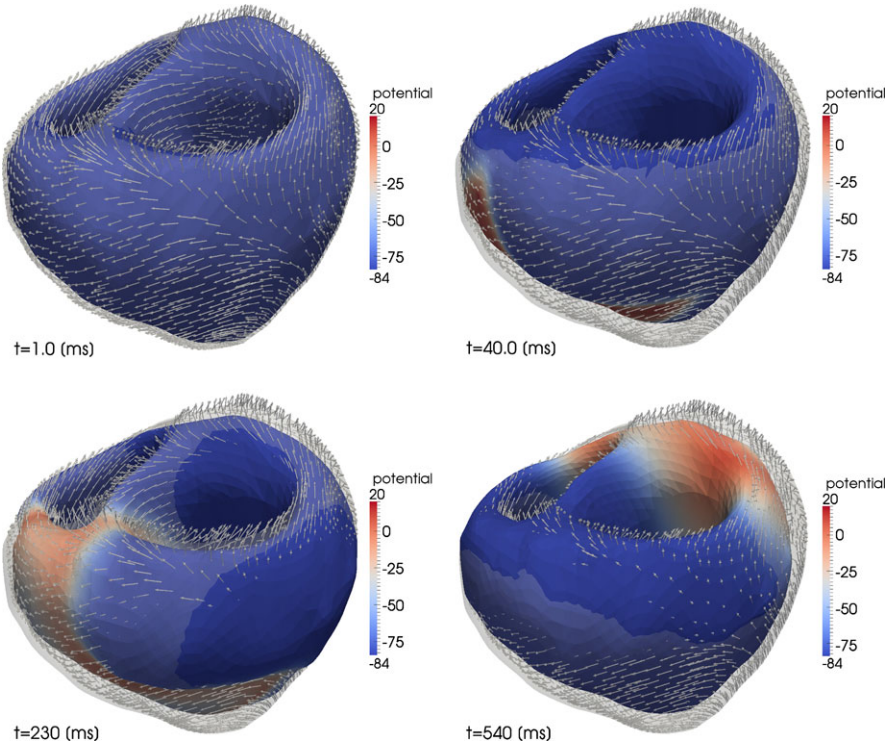

Fig. 14.4 Snapshots of the transmembrane potential field, plotted on the deformed configuration, and fiber distribution at times $t = 1, 40, 230, 540$ ms, plotted on the undeformed configuration

14.5 Conclusions and Future Directions

The material outlined in this paper reports some recent work in modeling and numerical simulation of cardiac electromechanics using the active strain approach. Even though several physical approximations apply, recently performed comparisons with experimental observations by Evangelista et al. (2011) (in terms of torsion of the left ventricle, endocardial volumes, and circumferential strains) and by Rossi et al. (2012) (in terms of end-systolic normal and shear strains) suggest the potential effectiveness of active-strain based models.

The effectiveness of an electromechanical model in capturing the key aspects of the physiology depends on several factors. In particular, we take electric models from a cell level and incorporate them in a force balance equation that holds at the macroscale. Yet, it is not obvious that such an uplift between spatial scales can be directly operated, without a suitable homogenization procedure. This is a concern shared by all current models of cardiac electromechanics, and needs to be addressed in further detail.

Acknowledgements The support by the European Research Council through the grant 'Mathcard, Mathematical Modelling and Simulation of the Cardiovascular System', ERC-2008-AdG 227058 is gratefully acknowledged.

References

Ambrosi D, Pezzuto S (2012) Active strain vs. active stress in mechanobiology: constitutive issues. J Elast 107:121–199

Ambrosi D, Arioli G, Nobile F, Quarteroni A (2011) Electromechanical coupling in cardiac dynamics: the active strain approach. SIAM J Appl Math 71:605–621

Ashikaga H, Coppola BA, Yamazaki KG, Villarreal FJ, Omens JH, Covell JW (2008) Changes in regional myocardial volume during the cardiac cycle: implications for transmural blood flow and cardiac structure. Am J Physiol, Heart Circ Physiol 295:H610–H618

Bueno-Orovio A, Cherry EM, Fenton FH (2008) Minimal model for human ventricular action potential in tissue. J Theor Biol 253:544–560

CellML (2000) (Language for storing and exchange of computer-based mathematical models). www.cellml.org

Chapelle D, Fernandez MA, Gerbeau JF, Moireau P, Sainte-Marie J, Zemzemi N (2009) Numerical simulation of the electromechanical activity of the heart. Lect Notes Comput Sci 5528:357–365

Cherubini C, Filippi S, Nardinocchi P, Teresi L (2008) An electromechanical model of cardiac tissue: constitutive issues and electrophysiological effects. Prog Biophys Mol Biol 97:562–573

Colli Franzone P, Pavarino LF (2004) A parallel solver for reaction-diffusion systems in computational electro-cardiology. Math Models Methods Appl Sci 14:883–911

Continuity (2005) (A problem-solving environment for multi-scale modeling in bioengineering and physiology). www.continuity.ucsd.edu/Continuity

Costa KD, Holmes JW, McCulloch AD (2001) Modelling cardiac mechanical properties in three dimensions. Philos Trans R Soc Lond A 359:1233–1250

Evangelista A, Nardinocchi P, Puddu PE, Teresi L, Torromeo C, Varano V (2011) Torsion of the human left ventricle: Experimental analysis and computational modelling. Prog Biophys Mol Biol 107:112–121

Göktepe S, Kuhl E (2010) Electromechanics of the heart: a unified approach to the strongly coupled excitation-contraction problem. Comput Mech 45:227–243

Hodgkin AL, Huxley AF (1952) A quantitative description of membrane current and its application to conductance and excitation in nerve. J Physiol 117:500–544

Holzapfel GA, Ogden RW (2009) Constitutive modelling of passive myocardium: a structurally based framework for material characterization. Philos Trans R Soc Lond A 367:3445–3475

Iribe G, Helmes M, Kohl P (2007) Force-length relations in isolated intact cardiomyocytes subjected to dynamic changes in mechanical load. Am J Physiol, Heart Circ Physiol 292:H1487–H1497

Iyer V, Mazhari R, Winslow RL (2004) A computational model of the human left ventricular epicardial myocyte. Biophys J 87:1507–1525

Kerckhoffs RCP, Healy SN, Usyk TP, McCulloch AD (2006) Computational methods for cardiac electromechanics. Proc IEEE 94:769–783

Lafortune P, Arís R, Vázquez M, Houzeaux G (2012) Coupled parallel electromechanical model of the heart. Int J Numer Methods Biomed Eng 28:72–86

Land S, Niederer SA, Smith NP (2012) Efficient computational methods for strongly coupled cardiac electromechanics. IEEE Trans Biomed Eng 59:1219–1228

Lee EH, Liu DT (1967) Finite strain elastic-plastic theory with application to plane-wave analysis. J Appl Phys 38:17–27

LifeV (2001) (A parallel finite element library). www.lifev.org

Luo C, Rudy Y (1991) A model of the ventricular cardiac action potential: depolarization, repolarization, and their interaction. Circ Res 68:1501–1526

Menzel A, Waffenschmidt T (2009) A micro-sphere-based remodelling formulation for anisotropic biological tissues. Philos Trans R Soc Lond A 367:3499–3523
Murtada S, Kroon M, Holzapfel GA (2010) A calcium-driven mechanochemical model for prediction of force generation in smooth muscle. Biomech Model Mechanobiol 9:749–762
Nardinocchi P, Teresi L (2007) On the active response of soft living tissues. J Elast 88:27–39
Nash MP, Hunter PJ (2000) Computational mechanics of the heart. J Elast 61:113–141
Nash MP, Panfilov AV (2004) Electromechanical model of excitable tissue to study reentrant cardiac arrhythmias. Prog Biophys Mol Biol 85:501–522
Nobile F, Quarteroni A, Ruiz-Baier R (2012) An active strain electromechanical model for cardiac tissue. Int J Numer Methods Biomed Eng 28:52–71
Pathmanathan P, Whiteley JP (2009) A numerical method for cardiac mechanoelectric simulations. Ann Biomed Eng 37:860–873
Pathmanathan P, Chapman SJ, Gavaghan D, Whiteley JP (2010) Cardiac electromechanics: the effect of contraction model on the mathematical problem and accuracy of the numerical scheme. Q J Mech Appl Math 63:375–399
Pitt-Francis J, Pathmanathan P, Bernabeu MO, Bordas R, Cooper J, Fletcher AG, Mirams GR, Murray P, Osbourne JM, Walter A, Chapman SJ, Garny A, van Leeuwen IMM, Maini PK, Rodriguez B, Waters SL, Whiteley JP, Byrne HM, Gavaghan D (2009) Chaste: a test-driven approach to software development for biological modelling. Comput Phys Commun 180:2452–2471. www.cs.ox.ac.uk/chaste
Rausch MK, Dam A, Göktepe S, Abilez OJ, Kuhl E (2011) Computational modeling of growth: systemic and pulmonary hypertension in the heart. Biomech Model Mechanobiol 10:799–811
Reumann M, Fitch BG, Rayshubskiy A, Keller D, Seemann G, Dossel O, Pitman MC, Rice JJ (2009) Strong scaling and speedup to 16,384 processors in cardiac electro-mechanical simulations. Proc IEEE 09:2795–2798
Rice JJ, Wang F, Bers DM, de Tombe PP (2008) Approximate model of cooperative activation and crossbridge cycling in cardiac muscle using ordinary differential equations. Biophys J 95:2368–2390
Rogers JM, McCulloch AD (1994) A collocation-Galerkin finite element model of cardiac action potential propagation. IEEE Trans Biomed Eng 41:743–757
Rossi S, Ruiz-Baier R, Pavarino LF, Quarteroni A (2011) Active strain and activation models in cardiac electromechanics. In Brenn G, Holzapfel GA, Schanz M, Steinbach O (eds) Proc Appl Math Mech, vol 11, pp 119–120
Rossi S, Ruiz-Baier R, Pavarino LF, Quarteroni A (2012) Orthotropic active strain models for the numerical simulation of cardiac biomechanics. Int J Numer Methods Biomed Eng 28:761–788
Rudy Y, Silva JR (2006) Computational biology in the study of cardiac ion channels and cell electrophysiology. Q Rev Biophys 39:57–116
Sermesant M (2003) Modèle électromécanique du coeur pour l'analyse d'image et la simulation. PhD Thesis, Université de Nice Sophia Antipolis, France
Smerup M, Nielsen E, Agger P, Frandsen J, Vestergaard-Poulsen P, Andersen J, Nyengaard J, Pedersen M, Ringgaard S, Hjortdal V, Lunkenheimer PP, Anderson RH (2009) The three-dimensional arrangement of the myocytes aggregated together within the mammalian ventricular myocardium. Anat Rec 292:1–11
Smith NP, Nickerson DP, Crampin EJ, Hunter PJ (2004) Multiscale computational modelling of the heart. Acta Numer 13:371–431
Taber LA, Perucchio R (2000) Modeling heart development. J Elast 61:165–197
ten Tusscher KH, Noble D, Noble PJ, Panfilov AV (2004) A model for human ventricular tissue. Am J Physiol, Heart Circ Physiol 286:H1573–H1589
Tung L (1978) A bi-domain model for describing ischemic myocardial D-C potentials. PhD Thesis, MIT, Cambridge, MA
Usyk TP, Mazhari R, McCulloch AD (2000) Effect of laminar orthotropic myofiber architecture on regional stress and strain in the canine left ventricle. J Elast 61:143–164